



RESEARCH ARTICLE | AUGUST 21 2023

## Chimeras in phase oscillator networks locally coupled through an auxiliary field: Stability and bifurcations

Special Collection: [Chimera states: from theory and experiments to technology and living systems](#)

Carlo R. Laing  



Chaos 33, 083141 (2023)

<https://doi.org/10.1063/5.0156627>



**Chaos**  
Special Topic:  
Anomalous Diffusion and Fluctuations  
in Complex Systems and Networks  
[Submit Today](#)



# Chimeras in phase oscillator networks locally coupled through an auxiliary field: Stability and bifurcations

Cite as: Chaos 33, 083141 (2023); doi: 10.1063/5.0156627

Submitted: 1 May 2023 · Accepted: 3 August 2023 ·

Published Online: 21 August 2023




View Online



Export Citation



CrossMark

Carlo R. Laing<sup>a)</sup> 

## AFFILIATIONS

School of Mathematical and Computational Sciences, Massey University, Private Bag 102-904 NSMC, Auckland, New Zealand

**Note:** This paper is part of the Focus Issue on Chimera states: from theory and experiments to technology and living systems.

<sup>a)</sup> Author to whom correspondence should be addressed: [c.r.laing@massey.ac.nz](mailto:c.r.laing@massey.ac.nz). Telephone: +64-9-414 0800, extension 43512.

Fax: +64-9-443 9790

## ABSTRACT

We study networks in the form of a lattice of nodes with a large number of phase oscillators and an auxiliary variable at each node. The only interactions between nodes are nearest-neighbor. The Ott/Antonsen ansatz is used to derive equations for the order parameters of the phase oscillators at each node, resulting in a set of coupled ordinary differential equations. Chimeras are steady states of these equations, and we follow them as parameters are varied, determining their stability and bifurcations. In two-dimensional domains, we find that spiral wave chimeras and rotating waves have significantly different properties than those in networks with nonlocal coupling.

© 2023 Author(s). All article content, except where otherwise noted, is licensed under a Creative Commons Attribution (CC BY) license (<http://creativecommons.org/licenses/by/4.0/>). <https://doi.org/10.1063/5.0156627>

**Chimeras are unusual spatiotemporal patterns in networks of oscillators characterized by having some oscillators synchronized, while the remainder are incoherent. Many studies of chimeras involve networks with nonlocal coupling, while a few consider only local coupling. Most of the studies of locally coupled networks show just the results of numerical simulations. We consider networks of phase oscillators with local interactions through an auxiliary field. Using the Ott/Antonsen ansatz, we derive and study equations for the dynamics of such networks, determining the stability and bifurcations of chimera states. In several cases, we find fundamental differences between solutions in locally coupled and nonlocally coupled networks.**

## I. INTRODUCTION

Chimeras are spatiotemporal patterns in networks of oscillators for which some oscillators synchronize, while the others are incoherent, even though the oscillators are identical or statistically identical.<sup>1,2</sup> Such patterns have less symmetry than the network which supports them. Chimeras have been studied intensively for more than a decade and observed in a number of physical systems.<sup>3,4</sup> One of the most significant advances in the study of chimeras was

the use of the Ott/Antonsen ansatz,<sup>5,6</sup> which gave an exact dimension reduction for infinite networks of sinusoidally coupled phase oscillators, such as the Kuramoto model;<sup>7,8</sup> for example, this ansatz allows one to describe the eventual dynamics of two coupled (infinite) networks by a pair of complex-valued ordinary differential equations.<sup>9,10</sup>

Chimeras were first reported in systems with nonlocal coupling,<sup>11-13</sup> and for some time, it was thought that such coupling was necessary in order that such states could be observed.<sup>14</sup> However, in 2015, Laing<sup>15</sup> showed numerically that chimeras could exist in systems with purely local coupling, considering three systems which could be thought of as approaching nonlocally coupled systems in a particular limit.

Since this first report of chimeras in systems with purely local coupling,<sup>15</sup> many other authors have reported chimeras in systems with only local coupling.<sup>16-19</sup> Some have studied systems where each node in isolation has complex dynamics (e.g., bursting<sup>20</sup>) or is bistable.<sup>21-23</sup> Others have considered reaction-diffusion type systems<sup>24-26</sup> similar to those whose analysis gave rise to early observations of chimeras.<sup>11,13</sup> However, all of these previous papers have shown just the results of numerically integrating the equations describing a dynamical system for a finite amount of time. While the accuracy of numerical integration can be controlled, there is the

possibility that some of the observed chimeras may actually be long-lived transients.<sup>27</sup> Any exploration of parameter space has resulted in fairly coarse partitioning of that space based on the stable patterns observed (often with no or limited exploration of dependence on initial conditions), and no analysis of the bifurcations creating or destroying chimeras has been undertaken.

To overcome these issues, here, we revisit several of the models in Ref. 15 and show that they can be analyzed using the Ott/Antonsen ansatz, which can be used to determine the stability of the chimeras found there, not just their existence. Such solutions can be followed as parameters are varied, and bifurcations of them characterized. We also consider a two-dimensional network with only local coupling, which supports spiral wave chimeras, and an annular domain which supports rotating waves, which have similarities to spiral wave chimeras.

All of the models studied here have a common form: the network is formed from a lattice of nodes, and at each node, there is a large number of phase oscillators and a single auxiliary variable, which may be real or complex. The phase oscillators at a node are influenced by the value of the auxiliary variable, which in turn is driven by some form of average over the states of the phase oscillators. The only interactions between nodes are nearest-neighbor, involving only the auxiliary variables. A number of other authors have considered networks of oscillators interacting diffusively through a medium,<sup>28–31</sup> and we discuss some of them further below.

The structure of the paper is as follows. Section II considers a one-dimensional network of Kuramoto phase oscillators, as studied in Ref. 15. In Sec. II A, we consider asymmetric local coupling in this model, which results in the chimera moving at a constant speed. In Sec. III, we consider Winfree oscillators on a one-dimensional domain, as studied in Ref. 15. In Secs. IV and V, we consider Kuramoto oscillators on two-dimensional domains in the shapes of a square and an annulus, respectively.

## II. KURAMOTO OSCILLATORS IN 1D

The first model we consider consists of  $N$  communities of oscillators equally spaced on a domain of length  $L$  with periodic boundary conditions, similar to that in Ref. 32. Each community consists of  $M$  phase oscillators and also has a complex variable  $z$  associated with it. The governing equations are

$$\frac{d\theta_j^k}{dt} = \omega_j^k - \text{Re} \left( z_j e^{-i\theta_j^k} \right), \quad (1)$$

$$\epsilon \frac{dz_j}{dt} = \frac{Ae^{i\beta}}{M} \sum_{k=1}^M e^{i\theta_j^k} - z_j + \frac{z_{j+1} - 2z_j + z_{j-1}}{(\Delta x)^2} \quad (2)$$

for  $j = 1, 2, \dots, N$  and  $k = 1, 2, \dots, M$ , where  $\theta_j^k$  is the phase of the  $k$ th oscillator in community  $j$ ,  $\Delta x = L/N$ , and  $A, \beta$ , and  $\epsilon$  are all constants. For each  $j$  and  $k$ ,  $\omega_j^k$  is randomly chosen from a Lorentzian distribution with half-width-at-half-maximum  $\sigma$  centered at  $\omega_0$ , namely,

$$g(\omega) = \frac{\sigma/\pi}{(\omega - \omega_0)^2 + \sigma^2}. \quad (3)$$

Thus, each phase oscillator in population  $j$  is influenced by the value of  $z_j$ , and  $z_j$  is driven by the mean over  $k$  of the  $e^{i\theta_j^k}$ , the classical Kuramoto order parameter. Note that the only coupling is nearest-neighbor between communities through the variable  $z$ . The last term in (2) is clearly a finite-difference approximation to  $\partial^2 z / \partial x^2$ .

An example of a chimera solution of (1) and (2) is shown in Fig. 1. For simplicity, the phase of only one phase oscillator in each community is shown. The phases  $\theta_j^1$  have clearly separated into a largely synchronous group and an asynchronous group, characteristic of a chimera, while the  $z_j$  vary relatively smoothly in space over the whole domain. The time-averaged frequencies of the oscillators also vary smoothly in space, as required for a chimera (not shown).

Letting  $M \rightarrow \infty$ , we can use the Ott/Antonsen ansatz<sup>3,6</sup> to describe the dynamics of the phase oscillator density in each community. Defining

$$a_j = \lim_{M \rightarrow \infty} \frac{1}{M} \sum_{k=1}^M e^{i\theta_j^k} \quad (4)$$

and then using standard calculations,<sup>1</sup> we have

$$\frac{da_j}{dt} = -(\sigma - i\omega_0)a_j - (i/2) \left( z_j + \bar{z}_j a_j^2 \right) \quad (5)$$

and (2) becomes

$$\epsilon \frac{dz_j}{dt} = Ae^{i\beta} a_j - z_j + \frac{z_{j+1} - 2z_j + z_{j-1}}{(\Delta x)^2}. \quad (6)$$

As explained in Ref. 15, the motivation for studying (1) and (2) comes from considering the case  $\epsilon = 0$ . If  $a_j$  is the  $j$ th entry of the vector  $\mathbf{a}$  and similarly for  $z_j$ , setting  $\epsilon = 0$  in (6) allows us to solve for  $\mathbf{z}$  in terms of  $\mathbf{a}$ ,

$$\mathbf{z} = Ae^{i\beta} (I - D)^{-1} \mathbf{a}, \quad (7)$$

where  $I$  is the  $N \times N$  identity matrix and  $D$  is the classical second difference operator on  $N$  points with periodic boundary conditions. The matrix  $(I - D)^{-1}$  can be found explicitly and has no non-zero entries, and inserting (7) into (5), we obtain an equation for the  $a_j$  with nonlocal coupling.

Equations (1) and (2) are invariant under a shift of all  $\theta_j^k$  by a constant and rotation of all  $z_j$  in the complex plane by the same amount, and thus, we go to a uniformly rotating coordinate frame in which the solutions of (5) and (6) of interest (chimeras) are stationary. Letting  $b_j = a_j e^{-i\Omega t}$  and  $y_j = z_j e^{-i\Omega t}$ , where  $\Omega$  is the (unknown) speed of rotation, we obtain

$$\frac{db_j}{dt} = -(\sigma - i(\omega_0 - \Omega))b_j - (i/2) \left( y_j + \bar{y}_j b_j^2 \right), \quad (8)$$

$$\epsilon \frac{dy_j}{dt} = Ae^{i\beta} b_j - y_j + \frac{y_{j+1} - 2y_j + y_{j-1}}{(\Delta x)^2} - i\epsilon \Omega y_j. \quad (9)$$

We are interested in steady states of these equations. An example is shown in Fig. 2 for the same parameters as used in Fig. 1.  $b_j$  and  $y_j$  are smooth functions of the spatial index  $j$ . Recall the interpretation of  $|b_j|$ : it is equal to  $|a_j|$  (4), and  $|b_j| = 1$  corresponds to synchronous oscillators (the distribution of phases is a Dirac delta function), while  $|b_j| = 0$  corresponds to a uniform angular distribution of phases, i.e.,

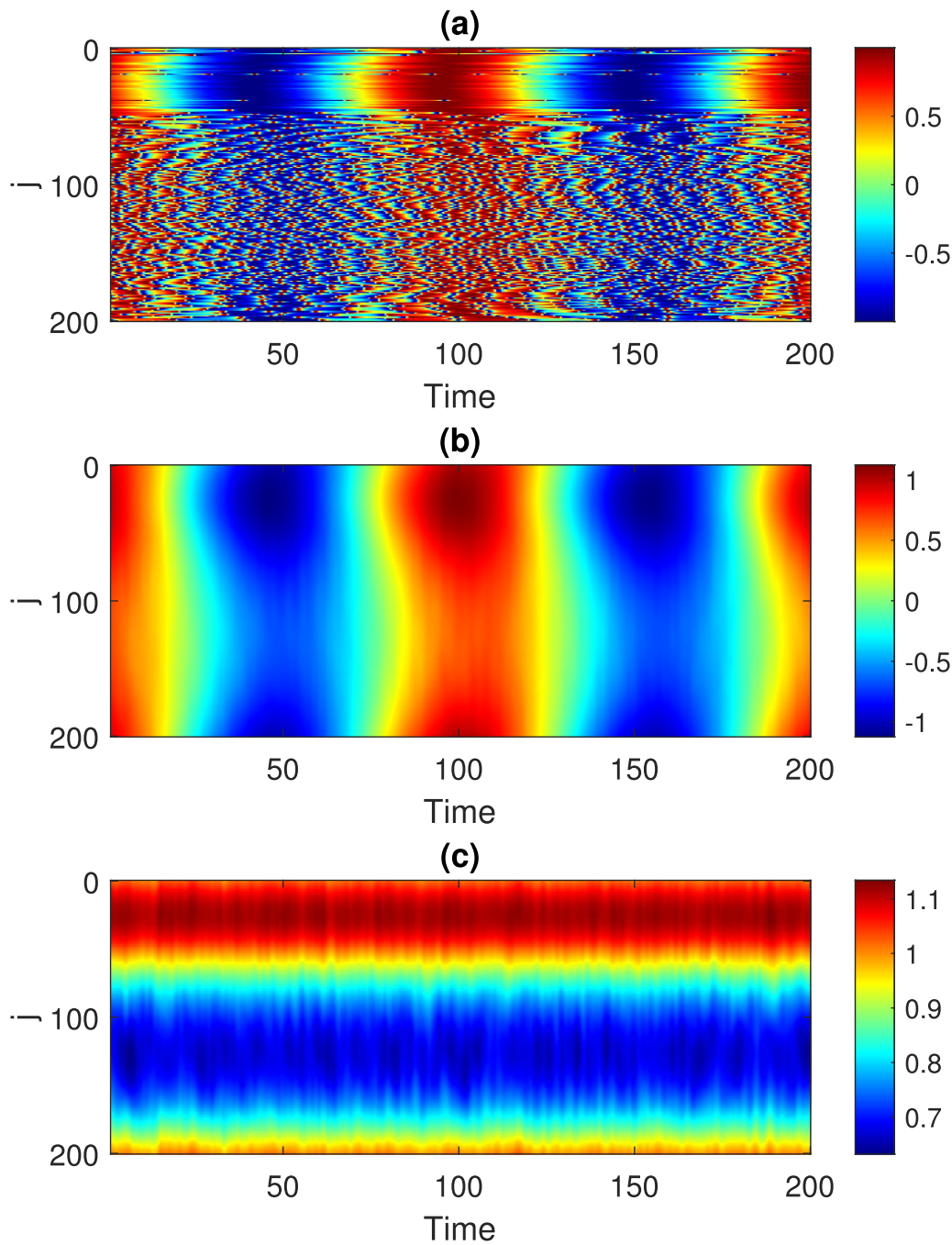


**FIG. 1.** Chimera solution of the system (1) and (2). (a)  $\sin \theta_j^1$ , (b)  $\sin(\arg(z_j))$ , and (c)  $|z_j|$ . Parameters:  $\omega_0 = 1, \sigma = 0.01, \epsilon = 0.2, A = 1.5, L = 2\pi, N = 200, M = 20, \beta = 0.1$ .

complete asynchrony. Due to the frequency heterogeneity in the network, i.e., the nonzero value of  $\sigma$ ,  $|b_j|$  never reaches 1, but the plateau centered at  $j = 100$  in Fig. 2 corresponds to the largely synchronous group seen for values of  $j$  centered at  $j \approx 30$  in Fig. 1(a).

We could find the steady state of (8) and (9) by setting the right hand side of (8) to zero and solving the resulting quadratic in  $b_j$  (choosing the solution for which  $|b_j| \leq 1$ ), then setting the right hand side of (9) to zero and inserting the value of  $b_j$  just found. This

22 August 2024 02:28:57

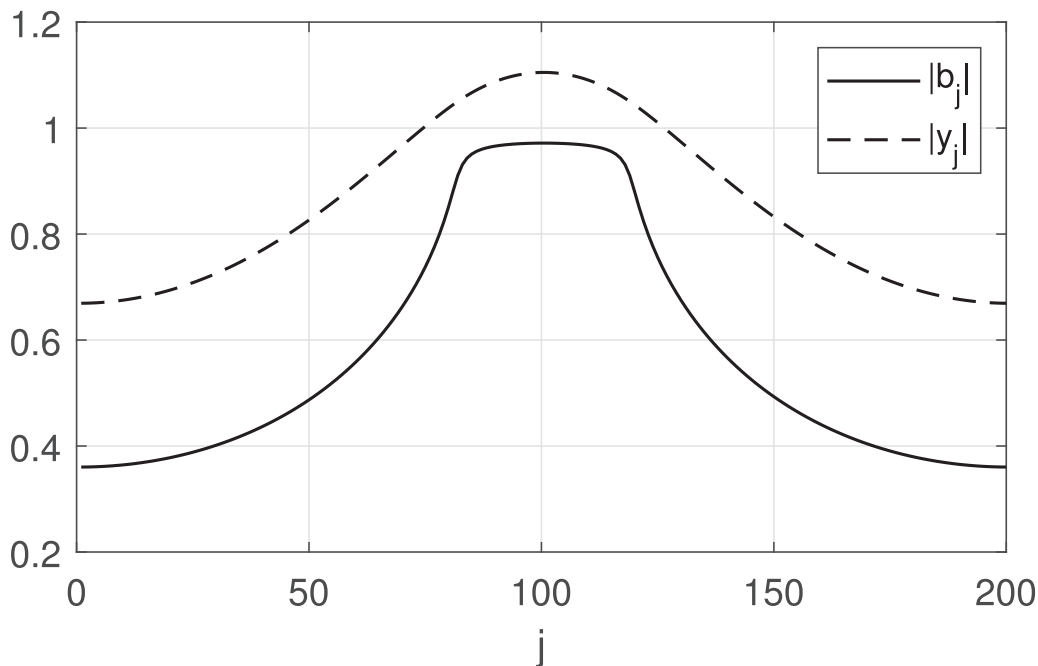


FIG. 2. Steady state of (8) and (9) with  $\Omega = -0.049437$ . Parameters as in Fig. 1.

gives an equation equivalent to Eq. (15) in Ref. 15. However, that is an equation just characterizing a steady state, if it exists, and gives no information about the stability of this solution. In contrast, here, we linearize (8) and (9) about such a steady state in order to determine its stability.

We explore the effects of varying both  $\epsilon$  and  $\beta$ . Increasing either  $\epsilon$  or  $\beta$  from the values used in Fig. 1, we find that the stable chimera is destroyed in a saddle-node bifurcation. Following this bifurcation as both  $\epsilon$  and  $\beta$  are varied, we obtain the blue solid curve in Fig. 3. The stable chimera also undergoes a Hopf bifurcation, which, from numerical simulations of (8) and (9), seems to be subcritical. The curve of Hopf bifurcations is shown dashed red in Fig. 3. Moving away from the nonlocally coupled case (i.e., increasing  $\epsilon$ ), the range of  $\beta$  values for which a chimera exists decreases.

In recent work,<sup>29</sup> Bolotov *et al.* studied equations equivalent to (5) and (6), although they considered identical oscillators so that  $\sigma = 0$  and also took the limit  $N \rightarrow \infty$ . They were interested in chimera solutions, which are spatially inhomogeneous steady states of (8) and (9) and showed that such states satisfy several spatial ordinary differential equations (once the limit  $N \rightarrow \infty$  has been taken). However, finding the stability of such states by linearizing (8) and (9) about them was difficult due to the large number of eigenvalues near the imaginary axis resulting from their consideration of identical oscillators. Instead, stability was inferred from the results of long simulations of the equivalent of (1) and (2).

Smirnov *et al.*<sup>30</sup> also considered equations equivalent to (5) and (6), also with  $\sigma = 0$  and in the limit  $N \rightarrow \infty$ . They showed that stable chimera solitons exist on an infinite domain, and these are described by homoclinic orbits in the spatial dynamics. They

also considered a spatially discrete model equivalent to (1) and (2) with  $M = 1$  and all  $\omega_j^k$  equal and found that the spatial discreteness caused the chimera solitons to move in an unusual “swaying” motion.

In earlier work,<sup>33</sup> Smirnov *et al.* considered equations equivalent to (5) and (6) but with  $\epsilon = 0$ , which, as explained above, corresponds to nonlocal coupling of the  $a_j$ . They studied solitary synchronization waves for which the local synchronization level is higher than in the surrounding background.

### A. Asymmetric coupling

The model (1) and (2) has symmetric local coupling since the dynamics of  $z_j$  depend equally on both  $z_{j+1}$  and  $z_{j-1}$ . However, one could also consider asymmetric local coupling. As an example, we replace (2) by

$$\epsilon \frac{dz_j}{dt} = \frac{Ae^{i\beta}}{M} \sum_{k=1}^M e^{i\theta^k} - z_j + \frac{z_{j+1} - 2z_j + z_{j-1}}{(\Delta x)^2} + \nu \frac{z_j - z_{j-1}}{\Delta x}, \quad (10)$$

where  $\nu$  is a constant. Clearly, this new term is a finite-difference approximation to  $\partial z / \partial x$ . Setting  $\nu \neq 0$  causes chimeras to move. Letting both  $M$  and  $N$  tend to infinity, we obtain the equations

$$\frac{\partial a}{\partial t} = -(\sigma - i\omega_0)a - (i/2)(z + \bar{z}a^2), \quad (11)$$

$$\epsilon \frac{\partial z}{\partial t} = Ae^{i\beta}a - z + \frac{\partial^2 z}{\partial x^2} + \nu \frac{\partial z}{\partial x}, \quad (12)$$

where  $a$  and  $z$  are now functions of  $x$  and  $t$ .

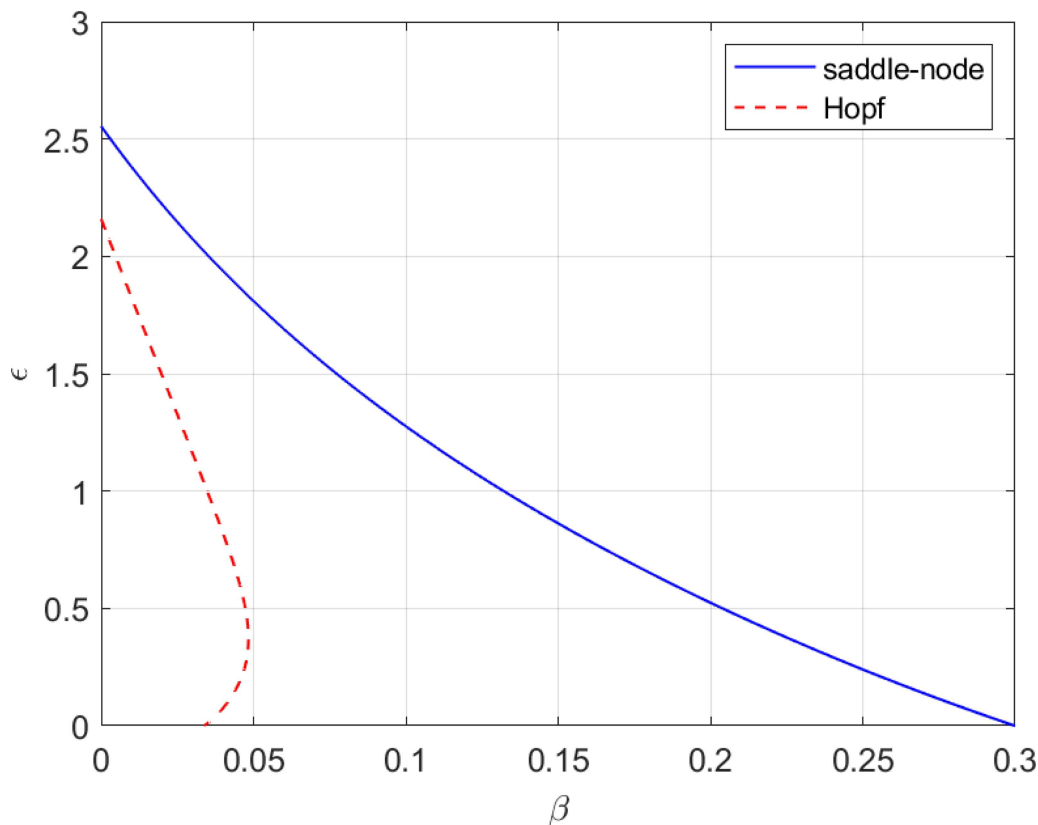


**FIG. 3.** Bifurcations of chimera steady states of (8) and (9). The chimera is stable within the region bounded by the two curves. Parameters:  $\omega_0 = 1, \sigma = 0.01, A = 1.5, L = 2\pi, N = 200$ .

The solutions of interest are chimeras, which move at a constant speed in  $x$ . We can freeze these moving solutions by going to a coordinate frame which is simultaneously translating at the speed of the chimeras and rotating at the same speed at each value of  $x$ .<sup>34,35</sup> If  $c$  is the speed at which a chimera is moving and  $s$  is the speed of the rotating coordinate frame, then in this new coordinate frame, (11) and (12) become

$$\frac{\partial a}{\partial t} = -(\sigma - i(\omega_0 - s))a - (i/2)(z + \bar{z}a^2) - c \frac{\partial a}{\partial x}, \quad (13)$$

$$\epsilon \frac{\partial z}{\partial t} = Ae^{i\beta}a - z + \frac{\partial^2 z}{\partial x^2} + (v - \epsilon c) \frac{\partial z}{\partial x} - i\epsilon sz. \quad (14)$$

We are interested in steady states of these equations. To solve them, we need to add several “pinning” conditions to remove the invariance of solutions under both spatial translations and rotations of  $a$  and  $z$  in the complex plane.<sup>34</sup> We can find the stability of these steady states by linearizing (13) and (14) about them.

Following a chimera steady state of (13) and (14) as  $v$  is varied, we obtain the plot shown in Fig. 4(a). For small  $v$ , the speed of the moving chimera initially increases as  $v$  does, but for

larger values, the plot of  $c$  vs  $v$  becomes multivalued. This phenomenon was first observed in Ref. 35 (see also Refs. 36–38). Moving chimeras are stable for small  $v$  but become unstable through a Hopf bifurcation at  $v \approx 0.3$ . This is in contrast to the moving chimeras in the nonlocally coupled system studied in Ref. 35, which lose and regain stability repeatedly as the branch of solutions is followed. Panels (b) and (c) of Fig. 4 show examples of profiles of  $|a(x, t)|$  for stable and unstable, respectively, moving chimeras. As in Refs. 35 and 37, the magnitude of  $a$  (i.e., the local level of synchrony of the phase oscillators) oscillates as one moves around the domain.

The traveling chimeras have an integer “twist” associated with them since as the domain is traversed once, the argument of  $a$  must vary through an integer multiple of  $2\pi$ . The twist of solutions on the curve shown in Fig. 4(a) starts at zero for small  $v$  and increases to 1 and 2 as  $v$  is increased (not shown).

In recent work,<sup>31</sup> Smirnov and Pikovsky considered a model equivalent to (1) and (10), but with identical oscillators,  $M = 1$  and  $N \rightarrow \infty$ . They set  $\epsilon = 0$ , which then creates *asymmetric* nonlocal coupling among the phase oscillators, similar to that in Refs. 35 and 37. They found traveling waves with varying twists and determined their stability and also patterns described as traveling chimeras.

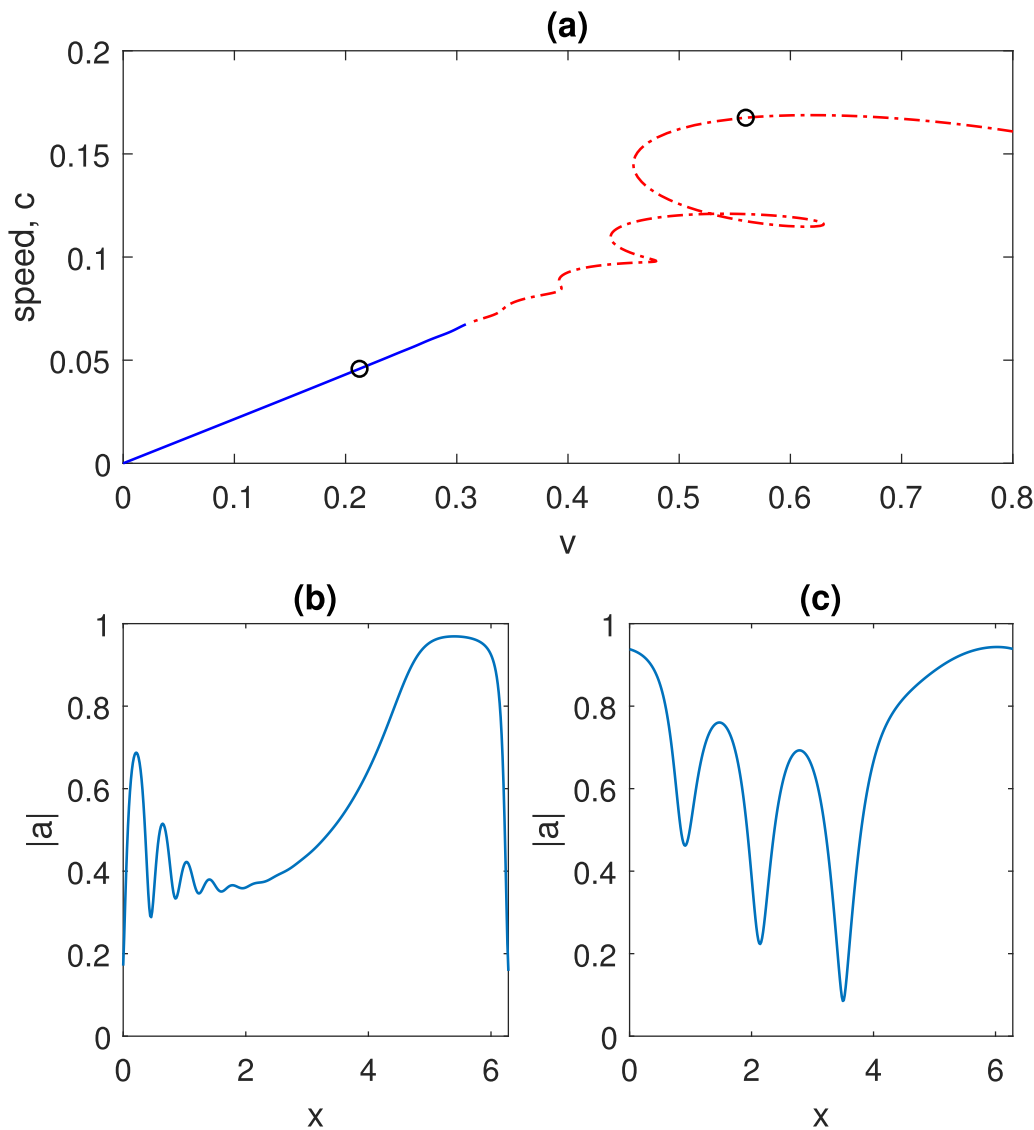


**FIG. 4.** (a) Speed,  $c$ , of the traveling chimera solution of (11) and (12) as a function of the magnitude of the asymmetric coupling,  $v$ . Blue solid: stable; red dashed–dotted: unstable. (b) and (c) Snapshots of  $|a(x, t)|$  at the points indicated by the black circles (left and right, respectively) in panel (a). Both chimeras are moving to the left. Parameters:  $\omega_0 = 1, \beta = 0.1, \epsilon = 0.2, \sigma = 0.01, A = 1.5, L = 2\pi$ . The domain was discretized with 400 points.

### III. WINFREE OSCILLATORS IN 1D

As a second example, we consider a network of Winfree oscillators.<sup>39–41</sup> The equations are

$$\frac{d\theta_j^k}{dt} = \omega_j^k + \kappa Q(\theta_j^k)u_j, \tag{15}$$

$$\epsilon \frac{du_j}{dt} = \frac{1}{M} \sum_{k=1}^M P_n(\theta_j^k) - u_j + \frac{u_{j+1} - 2u_j + u_{j-1}}{(\Delta x)^2} \tag{16}$$

for  $j = 1, 2, \dots, N$  and  $k = 1, 2, \dots, M$ , where  $\theta_j^k$  is the phase of the  $k$ th oscillator in community  $j$ , and  $\kappa$  and  $\epsilon$  are parameters. Note that each  $u_j$  is real. The functions  $Q$  and  $P_n$  are given by  $Q(\theta) = \sin \beta - \sin(\theta + \beta)$ , where  $\beta$  is a parameter,  $P_n(\theta) = a_n(1 + \cos \theta)^n$  where  $a_n = 2^n(n!)^2/(2n)!$ , and  $\Delta x = L/N$ , where  $L$  is the length of the domain. Periodic boundary conditions in space are used.  $Q(\theta)$  is the phase response curve of the oscillator and can be measured experimentally for a neuron, for example.<sup>42</sup> As above,  $\omega_j^k$  are randomly chosen from the distribution (3).

An example of a chimera is shown in Fig. 5 where for simplicity, we show the phase of only one oscillator at each lattice

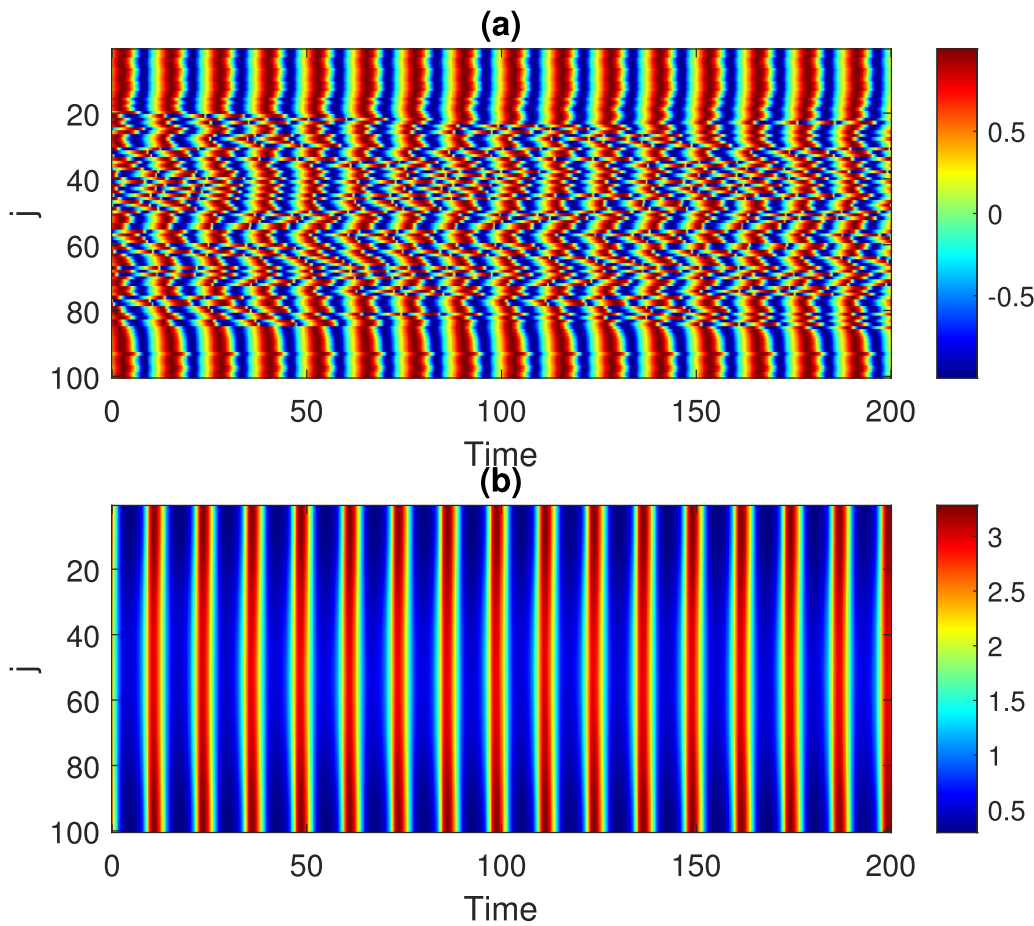


FIG. 5. Chimera state in (15) and (16). (a)  $\sin \theta_j^1$  and (b)  $u_j$ . Parameters:  $\omega_0 = 0.3, \beta = \pi/2 - 0.2, \kappa = 0.4, \epsilon = 0.1, \sigma = 0.001, n = 4, M = 20, N = 100, L = 4$ .

point. The incoherent group of oscillators is in the center of the domain. A chimera in such a system was shown in Ref. 15, but no analysis of it was performed.

As above, we can let  $M \rightarrow \infty$  and use the Ott/Antonsen ansatz to derive equations describing the phase oscillator density in each community. Defining  $a_j$  as in (4), we find<sup>43</sup>

$$\frac{da_j}{dt} = \kappa u_j e^{-i\beta} / 2 + (i\omega_0 - \delta + i\kappa \sin(\beta) u_j) a_j - \kappa e^{i\beta} u_j a_j^2 / 2. \quad (17)$$

Setting  $n = 4$ , we find that<sup>44</sup>

$$\lim_{M \rightarrow \infty} \frac{1}{M} \sum_{k=1}^M P_n(\theta_j^k) = 1 + \frac{4(a_j + \bar{a}_j)}{5} + \frac{2(a_j^2 + \bar{a}_j^2)}{5} + \frac{4(a_j^3 + \bar{a}_j^3)}{35} + \frac{a_j^4 + \bar{a}_j^4}{70} \equiv f(a_j, \bar{a}_j),$$

and thus, the system is described by (17) and

$$\epsilon \frac{du_j}{dt} = f(a_j, \bar{a}_j) - u_j + \frac{u_{j+1} - 2u_j + u_{j-1}}{(\Delta x)^2}. \quad (18)$$

Unlike the system studied in Sec. II, Eqs. (15) and (16) are not invariant under a uniform rotation of phases, and thus, the chimera shown in Fig. 5 corresponds to a periodic solution of (17) and (18) and must be studied as such.

One of the important parameters in a network of Winfree oscillators is the level of heterogeneity in natural frequencies, given here by  $\delta$ . Varying  $\delta$  and following both fixed points and periodic solutions of (17) and (18), we obtain Fig. 6. As in an all-to-all coupled network, for small  $\kappa$  and large  $\delta$ , the system has a stable spatially uniform fixed point, indicated by the solid blue curve. As  $\delta$  is decreased, this state loses stability in a supercritical Hopf bifurcation, leading to a stable periodic solution, again with no spatial structure (shown with blue circles). As  $\delta$  is decreased further, this state loses stability to a solution which is periodic in time and which has some spatial structure: this is the chimera state corresponding to the type of solution shown in Fig. 5.

To represent the chimera, we define a chimera index

$$\chi \equiv \frac{1}{T} \int_0^T \max_x (u(x, t)) - \min_x (u(x, t)) dt, \quad (19)$$

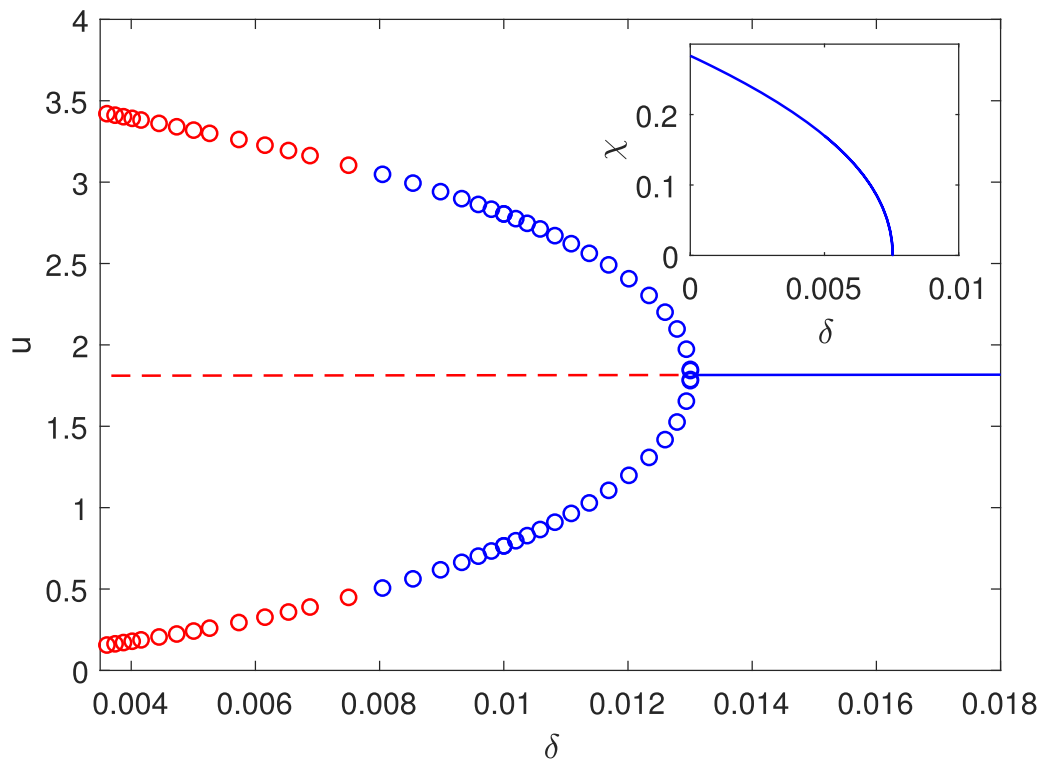


**FIG. 6.** Fixed points and periodic solutions of (17) and (18). Lines show the value of  $u$  at a spatially uniform fixed point (solid blue: stable; dashed red: unstable). Circles show the maximum and minimum of  $u$  over one period of a spatially uniform periodic solution (blue: stable; red: unstable). The inset shows the chimera index  $\chi$  defined in the text. Parameters:  $\omega_0 = 0.3$ ,  $\beta = \pi/2 - 0.2$ ,  $\kappa = 0.4$ ,  $\epsilon = 0.1$ ,  $n = 4$ ,  $M = 1$ ,  $N = 100$ ,  $L = 4$ .

where  $T$  is the period of the oscillation. For a spatially uniform periodic state,  $\chi$  will be zero. In the inset of Fig. 6, we plot  $\chi$  as a function of  $\delta$ . We see that  $\chi$  varies from 0 (at  $\delta \approx 0.0075$ ) when the spatially uniform period state loses stability to a maximum at  $\delta = 0$ ; i.e., the chimera bifurcates in a supercritical way. The chimera is stable over the range of  $\delta$  for which it exists.

Increasing  $\kappa$  with  $\delta = 0.005$  and all other parameters the same as above, we see the same scenario (not shown).

#### IV. 2D SQUARE DOMAIN

The next system we consider is a two-dimensional square domain. Spiral wave chimeras have been observed in a number of

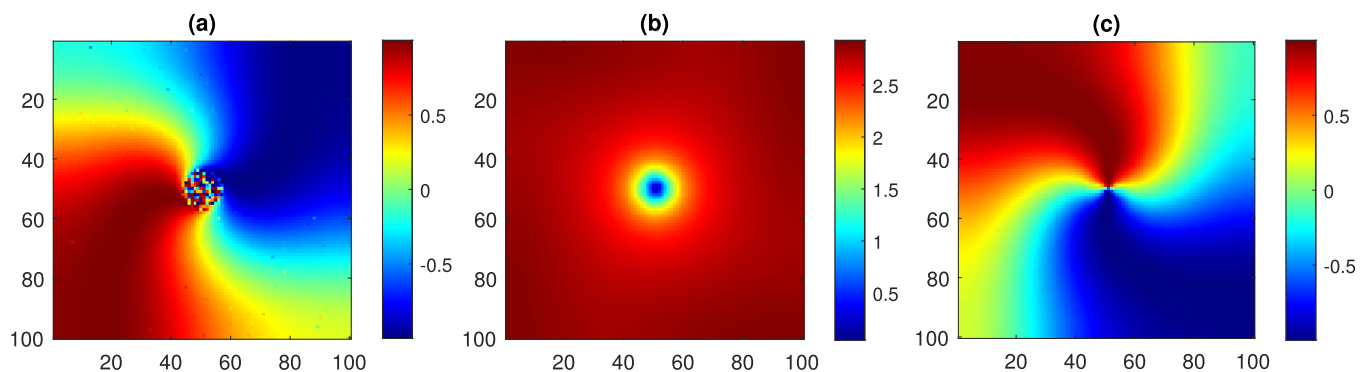


**FIG. 7.** Snapshot of a spiral wave chimera solution of (20) and (21). (a)  $\sin \theta_j^1$ , (b)  $|z_j|$ , and (c):  $\sin(\arg(z_j))$ . Parameters:  $\omega_0 = 0$ ,  $\alpha = 0.7\pi$ ,  $\sigma = 0.001$ ,  $\epsilon = 20$ ,  $M = 1$ ,  $N = 100$ ,  $L = 3$ .

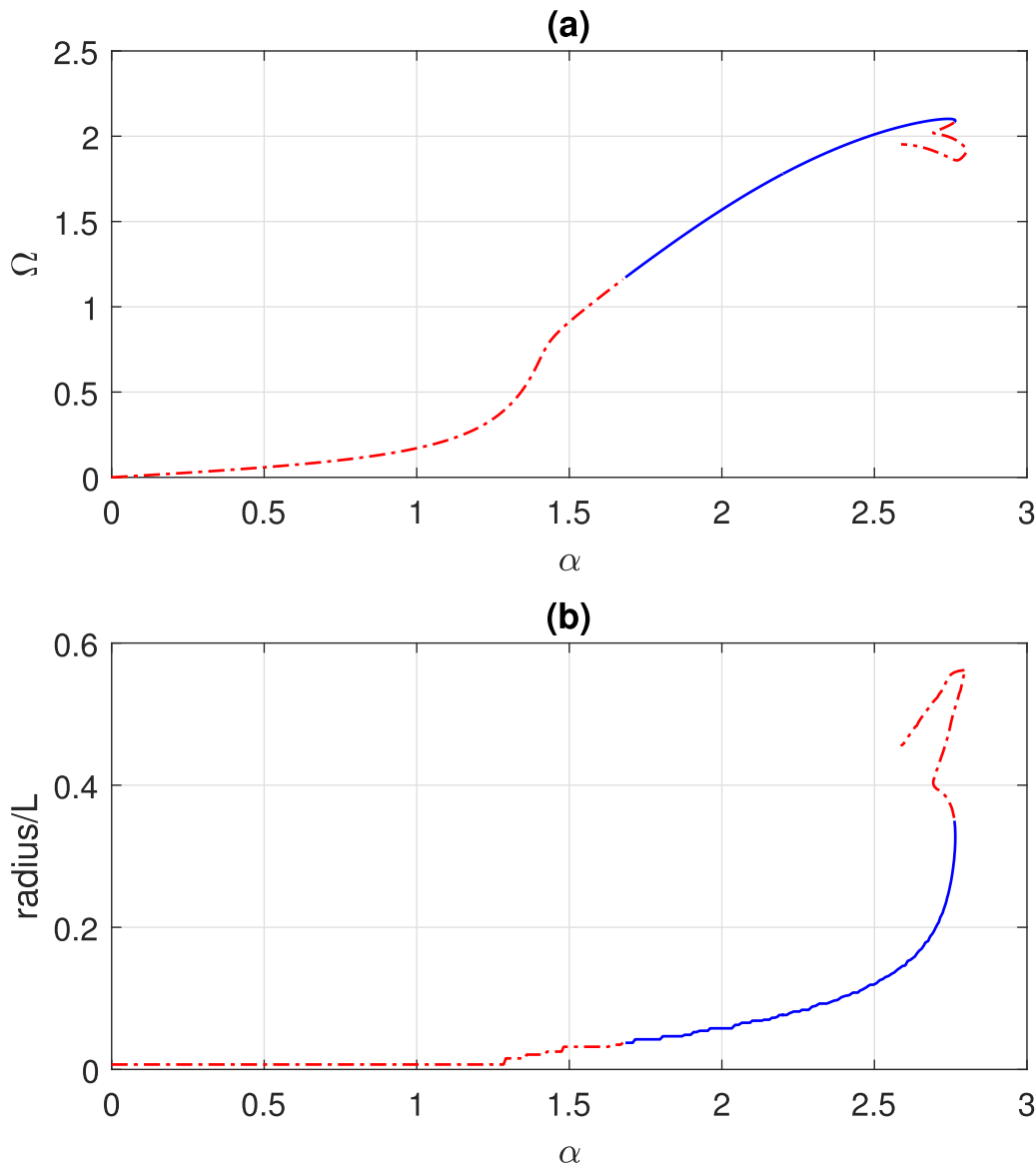


**FIG. 8.** Continuation in  $\alpha$  of a spiral wave chimera steady state of (22) and (23). (a)  $\Omega$  vs  $\alpha$ . (b) Radius of incoherent core, divided by domain side length  $L$ , vs  $\alpha$ . Blue solid: stable; red dashed–dotted: unstable. Parameters:  $\omega_0 = 0, \sigma = 0.03, \epsilon = 20, N = 81, L = 3$ .

two-dimensional networks with nonlocal coupling.<sup>45–47</sup> Our system is

$$\frac{d\theta_j^k}{dt} = \omega_j^k - \text{Im} \left[ e^{i(\theta_j^k + \alpha)} z_j \right] = \omega_j^k + (i/2) \left[ e^{i(\theta_j^k + \alpha)} z_j - e^{-i(\theta_j^k + \alpha)} \bar{z}_j \right], \tag{20}$$

$$\epsilon \frac{dz_j}{dt} = \frac{100}{M} \sum_{k=1}^M e^{-i\theta_j^k} + \nabla^2 z_j - z_j, \tag{21}$$

where as above,  $\theta_j^k$  is the phase of the  $k$ th oscillator in community  $j$  and  $j$  is the index of a point in a 2D lattice. We use a five-point stencil to approximate the Laplacian on a regular  $N \times N$  square grid and use zero-derivative Neumann boundary conditions. An example of a spiral wave chimera solution of (20) and (21) is shown in Fig. 7 where for simplicity, we set  $M = 1$ . In the image of  $\sin \theta_j^1$ , the incoherent core is clearly visible. There is slight “speckling” in panel (a) due to the randomly chosen values of  $\omega_j^1$ .  $z$  is clearly a smooth function of space with a phase singularity where  $|z| = 0$  at the center of the spiral.

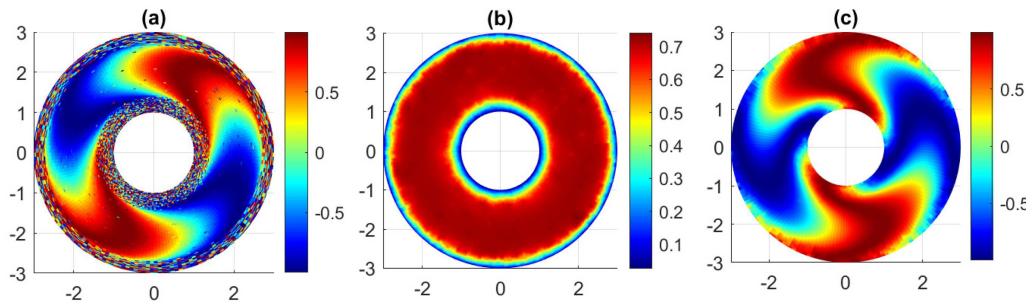


**FIG. 9.** Snapshot of a rotating wave solution of (24) and (25) with  $n = 2$ . (a)  $\sin \theta_j^1$ , (b)  $|z_j|$ , and (c)  $\sin(\arg(z_j))$ . Parameters:  $\omega_0 = 0, \alpha = 2.7, \sigma = 0.001, \epsilon = 100, M = 1, a = 1, b = 3, N_r = 100, N_\phi = 180$ .

Taking the limit  $M \rightarrow \infty$  and defining  $a_j$  to be the complex conjugate of the term on the right of (4), we have

$$\epsilon \frac{dz_j}{dt} = 100a_j + \nabla^2 z_j - z_j$$

and

$$\frac{da_j}{dt} = z_j e^{i\alpha} / 2 - (\sigma + i\omega_0)a_j - \bar{z}_j e^{-i\alpha} a_j^2 / 2.$$

The solutions of interest are stationary in a rotating coordinate frame; i.e., we are interested in fixed points of

$$\frac{da_j}{dt} = z_j e^{i\alpha} / 2 - (\sigma + i\omega_0)a_j - \bar{z}_j e^{-i\alpha} a_j^2 / 2 - i\Omega a_j, \quad (22)$$

$$\epsilon \frac{dz_j}{dt} = 100a_j + \nabla^2 z_j - z_j - \epsilon i\Omega z_j, \quad (23)$$

where  $\Omega$  is the speed of the rotating coordinate frame.

Following such a fixed point as  $\alpha$  is varied, we obtain the results in Fig. 8. One interesting result is that unlike other systems, the spiral persists for  $\alpha$  greater than  $\pi/2$ . Another interesting result is shown in panel (b) where the radius of the incoherent core is plotted. In other systems, this increased linearly with  $\alpha$ , at least for small  $\alpha$ . Here, the core does not really develop until  $\alpha \approx 1.3$ . (The incoherent core was defined as grid points for which  $|a_j| < 0.95$ . Since  $N$  is odd, there is always at least one lattice point, in the center of the spiral, for which  $|a_j| < 0.95$ , and thus, this radius is never zero.)

### V. ANNULUS

One type of domain on which chimeras have recently been studied is the annulus.<sup>48</sup> Laing previously investigated both multi-headed chimeras and rotating waves in networks of nonlocally coupled phase oscillators on an annulus.<sup>48</sup> (Also, see Ref. 49.)

The model we consider is

$$\frac{d\theta_j^k}{dt} = \omega_j^k - \text{Im} \left[ e^{i(\theta_j^k + \alpha)} z_j \right] = \omega_j^k + (i/2) \left[ e^{i(\theta_j^k + \alpha)} z_j - e^{-i(\theta_j^k + \alpha)} \bar{z}_j \right], \quad (24)$$

$$\epsilon \frac{dz_j}{dt} = \frac{50}{M} \sum_{k=1}^M e^{-i\theta_j^k} + \nabla^2 z_j - z_j, \quad (25)$$

where as above,  $\theta_j^k$  is the phase of the  $k$ th oscillator in community  $j$  and  $j$  is the index of a point on the annulus with inner radius  $a$  and outer radius  $b$ . The domain is discretized with  $N_r$  points in the radial direction and  $N_\phi$  in the angular direction. Second derivatives in the angular and radial directions were implemented as in (2), and the first derivative in the radial direction was implemented using a centered finite difference. Importantly, Dirichlet boundary conditions are used for  $z$ , where  $z = 0$  on both the inner and outer boundaries.

An example of a rotating wave solution of (24) and (25) is shown in Fig. 9. In the plot of  $\sin \theta_j^1$ , we see incoherent regions near the inner and outer boundaries of the domain, while  $\theta_j^1$  increases through  $4\pi$  as we move in the angular direction around the domain, away from the boundaries. The phase  $\theta_j^1$  will vary through a multiple of  $2\pi$  as we move around the domain, and in this case, that multiple is  $n = 2$ , referred to as the winding number. We see that  $z$  is continuous in space.

The reason for the oscillators near the boundaries being incoherent is easy to see: oscillators at point  $j$  feel the field  $z_j$ , and if  $|z_j|$  is small, the oscillators will not lock to it. Since  $z$  is continuous in space and equal to zero at the boundaries, there must be some incoherent oscillators near the boundaries.

As in Sec. IV, in the limit  $M \rightarrow \infty$ , the solutions of interest are fixed points of

$$\frac{da_j}{dt} = z_j e^{i\alpha} / 2 - (\sigma + i\omega_0)a_j - \bar{z}_j e^{-i\alpha} a_j^2 / 2 - i\Omega a_j, \quad (26)$$

$$\epsilon \frac{dz_j}{dt} = 50a_j + \nabla^2 z_j - z_j - \epsilon i\Omega z_j, \quad (27)$$

where  $\Omega$  is the speed of the rotating coordinate frame.

We followed rotating waves with  $n = 0, 1, 2, 3$  as  $\alpha$  was varied, and the results are shown in Fig. 10. Only the  $n = 0, 1$  curves persist down to  $\alpha = 0$ , others have saddle-node bifurcations. The  $n = 0$  curve is always stable, and the other curves are only stable for  $\sim 1.5 < \alpha < \sim 2.5$ . These results are fundamentally different in

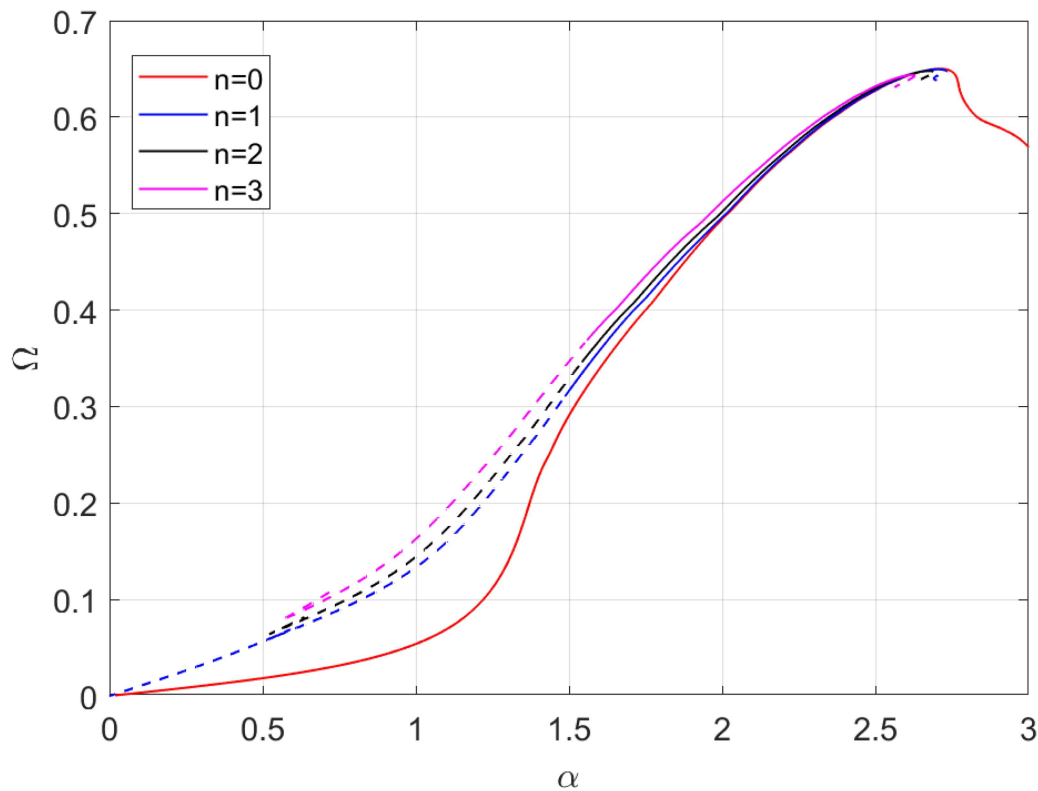


**FIG. 10.** Rotation speed  $\Omega$  as a function of  $\alpha$  for rotating waves with winding numbers  $n = 0, 1, 2, 3$ . Solid curves: stable; dashed: unstable. Parameters:  $\omega_0 = 0$ ,  $\sigma = 0.001$ ,  $\epsilon = 100$ ,  $M = 1$ ,  $a = 1$ ,  $b = 3$ .  $N_r = 60$ ,  $N_\phi = 100$ .

several ways from those for nonlocally coupled oscillators found in Ref. 48; here,

- the curves do not all persist down to  $\alpha = 0$ ,
- the curves persist past  $\alpha = \pi/2$ , and
- curves for different  $n$  are not simply related by scaling  $\Omega$  (and here, the value of  $\Omega$  increases with  $n$ , whereas in Ref. 48, it decreases).

## VI. SUMMARY

We studied a number of networks of phase oscillators where at each node, there are many phase oscillators and one auxiliary variable, which may be real or complex. The only coupling between nodes is nearest-neighbor coupling of the auxiliary variables. These networks are capable of supporting stable chimera states, for which oscillators in part of the domain are largely synchronous, while those in the rest are more asynchronous. All of these systems can be studied using the Ott/Antonsen ansatz applied to the phase oscillator populations, and we obtain a set of coupled equations for both the Kuramoto order parameter and the value of the auxiliary variable at each node. Steady states of these equations correspond to chimeras, and their stability and bifurcations can, thus, be determined straightforwardly.

We first examined several one-dimensional networks previously studied in Ref. 15, but now, we can properly determine the stability of chimeras found in those networks. For the Kuramoto oscillators (Sec. II), adding local asymmetric coupling caused the chimera to move around the domain. Interestingly, the chimera's speed is not a monotonic function of the asymmetric coupling strength, a phenomenon seen previously only in systems with non-local coupling.<sup>35–38</sup> For the Winfree oscillators (Sec. III), we showed how the chimera arises as the result of several bifurcations as the heterogeneity of the uncoupled oscillators' frequencies decreased. We then considered a spiral wave chimera in a square domain (Sec. IV). In contrast with many other spiral wave chimeras found in nonlocally coupled systems,<sup>46,47,50–52</sup> the spiral wave chimera found here (i) exists for  $\alpha$  significantly past  $\alpha = \pi/2$  and (ii) does not have a core whose size grows linearly with  $\alpha$  (for small  $\alpha$ ). The last system considered was an annular domain, for which we studied rotating waves. While these patterns do have some coherent and some incoherent oscillators, they should not be considered chimeras, as the incoherent oscillators are near the boundaries of the domain, where the auxiliary variable must have a small magnitude due to the boundary conditions.

For both two-dimensional domains (Secs. IV and V), we found that solutions of interest are fundamentally different in several ways from those for which coupling is nonlocal. These results add to our

knowledge of the types of dynamics seen in networks and invite further investigations into the similarities and differences in the dynamics of networks with local and nonlocal coupling.<sup>53</sup>

## AUTHOR DECLARATIONS

### Conflict of Interest

The authors have no conflicts to disclose.

### Author Contributions

**Carlo R. Laing:** Conceptualization (equal); Investigation (equal); Software (equal); Writing – original draft (equal); Writing – review & editing (equal).

### DATA AVAILABILITY

The data that support the findings of this study are available within the article.

## REFERENCES

- <sup>1</sup>O. E. Omel'chenko, "The mathematics behind chimera states," *Nonlinearity* **31**(5), R121 (2018).
- <sup>2</sup>M. J. Panaggio and D. M. Abrams, "Chimera states: Coexistence of coherence and incoherence in networks of coupled oscillators," *Nonlinearity* **28**(3), R67 (2015).
- <sup>3</sup>E. A. Martens, S. Thutupalli, A. Fourrière, and O. Hallatschek, "Chimera states in mechanical oscillator networks," *Proc. Natl. Acad. Sci. U.S.A.* **110**(26), 10563–10567 (2013).
- <sup>4</sup>J. F. Totz, J. Rode, M. R. Tinsley, K. Showalter, and H. Engel, "Spiral wave chimera states in large populations of coupled chemical oscillators," *Nat. Phys.* **14**(3), 282–285 (2018).
- <sup>5</sup>E. Ott and T. M. Antonsen, "Low dimensional behavior of large systems of globally coupled oscillators," *Chaos* **18**(3), 037113 (2008).
- <sup>6</sup>E. Ott and T. M. Antonsen, "Long time evolution of phase oscillator systems," *Chaos* **19**(2), 023117 (2009).
- <sup>7</sup>S. H. Strogatz, "From Kuramoto to Crawford: Exploring the onset of synchronization in populations of coupled oscillators," *Physica D* **143**(1–4), 1–20 (2000).
- <sup>8</sup>Y. Kuramoto, *Chemical Oscillations, Waves, and Turbulence* (Springer, Berlin, 1984).
- <sup>9</sup>D. M. Abrams, R. Mirollo, S. H. Strogatz, and D. A. Wiley, "Solvable model for chimera states of coupled oscillators," *Phys. Rev. Lett.* **101**(8), 084103 (2008).
- <sup>10</sup>C. R. Laing, "Chimera states in heterogeneous networks," *Chaos* **19**(1), 013113 (2009).
- <sup>11</sup>Y. Kuramoto and D. Battogtokh, "Coexistence of coherence and incoherence in nonlocally coupled phase oscillators," *Nonlinear Phenom. Complex Syst.* **5**(4), 380–385 (2002).
- <sup>12</sup>D. M. Abrams and S. H. Strogatz, "Chimera states in a ring of nonlocally coupled oscillators," *Int. J. Bifurcat. Chaos* **16**(1), 21–37 (2006).
- <sup>13</sup>Y. Kuramoto and S. Shima, "Rotating spirals without phase singularity in reaction-diffusion systems," *Progr. Theor. Phys. Suppl.* **150**, 115 (2003).
- <sup>14</sup>S. W. Haugland, "The changing notion of chimera states, a critical review," *J. Phys.: Complex.* **2**(3), 032001 (2021).
- <sup>15</sup>C. R. Laing, "Chimeras in networks with purely local coupling," *Phys. Rev. E* **92**(5), 050904 (2015).
- <sup>16</sup>Z. G. Nicolaou, H. Riecke, and A. E. Motter, "Chimera states in continuous media: Existence and distinctness," *Phys. Rev. Lett.* **119**, 244101 (2017).
- <sup>17</sup>M. G. Clerc, S. Coulibaly, M. A. Ferré, M. A. García-Nustes, and R. G. Rojas, "Chimera-type states induced by local coupling," *Phys. Rev. E* **93**(5), 052204 (2016).
- <sup>18</sup>V. García-Morales, J. A. Manzanares, and K. Krischer, "Chimera states under genuine local coupling," *Chaos, Solitons Fractals* **165**, 112808 (2022).
- <sup>19</sup>T. J. Kaper and T. Vo, "A new class of chimeras in locally coupled oscillators with small-amplitude, high-frequency asynchrony and large-amplitude, low-frequency synchrony," *Chaos* **31**(12), 123111 (2021).
- <sup>20</sup>B. K. Bera and D. Ghosh, "Chimera states in purely local delay-coupled oscillators," *Phys. Rev. E* **93**, 052223 (2016).
- <sup>21</sup>J. Hizanidis, N. Lazarides, and G. P. Tsironis, "Chimera states in networks of locally and non-locally coupled squids," *Front. Appl. Math. Stat.* **5**, 33 (2019).
- <sup>22</sup>M. G. Clerc, S. Coulibaly, M. A. Ferré, and R. G. Rojas, "Chimera states in a Duffing oscillators chain coupled to nearest neighbors," *Chaos* **28**(8), 083126 (2018).
- <sup>23</sup>D. S. Shchapin, A. S. Dmitrichev, and V. I. Nekorkin, "Chimera states in an ensemble of linearly locally coupled bistable oscillators," *JETP Lett.* **106**, 617–621 (2017).
- <sup>24</sup>B.-W. Li and H. Dierckx, "Spiral wave chimeras in locally coupled oscillator systems," *Phys. Rev. E* **93**(2), 020202 (2016).
- <sup>25</sup>X. Tang, T. Yang, I. R. Epstein, Y. Liu, Y. Zhao, and Q. Gao, "Novel type of chimera spiral waves arising from decoupling of a diffusible component," *J. Chem. Phys.* **141**(2), 024110 (2014).
- <sup>26</sup>L. Yang, Y. He, and B.-W. Li, "Spiral wave chimeras in populations of oscillators coupled to a slowly varying diffusive environment," *Front. Phys.* **18**(1), 13309 (2023).
- <sup>27</sup>A. Zakharova, *Chimera Patterns in Networks* (Springer, 2020).
- <sup>28</sup>S. Choe, I.-H. Pak, H. Jang, R.-S. Kim, and C.-U. Choe, "Self-emerging symmetry breakings in a two-population network of phase oscillators interacting via an external environment," *Phys. D* **440**, 133483 (2022).
- <sup>29</sup>D. I. Bolotov, M. I. Bolotov, L. A. Smirnov, G. V. Osipov, and A. S. Pikovsky, "Synchronization regimes in an ensemble of phase oscillators coupled through a diffusion field," *Radiophys. Quantum Electron.* **64**(10), 709–725 (2022).
- <sup>30</sup>L. A. Smirnov, M. I. Bolotov, D. I. Bolotov, G. V. Osipov, and A. S. Pikovsky, "Finite-density-induced motility and turbulence of chimera solitons," *New J. Phys.* **24**(4), 043042 (2022).
- <sup>31</sup>L. Smirnov and A. Pikovsky, "Travelling chimeras in oscillator lattices with advective-diffusive coupling," *Philos. Trans. R. Soc. A* **381**(2245), 20220076 (2023).
- <sup>32</sup>C. R. Laing, "Chimeras on a ring of oscillator populations," *Chaos* **33**(1), 013121 (2023).
- <sup>33</sup>L. A. Smirnov, G. V. Osipov, and A. Pikovsky, "Solitary synchronization waves in distributed oscillator populations," *Phys. Rev. E* **98**, 062222 (2018).
- <sup>34</sup>C. R. Laing, "Fronts and bumps in spatially extended Kuramoto networks," *Physica D* **240**(24), 1960–1971 (2011).
- <sup>35</sup>O. E. Omel'chenko, "Travelling chimera states in systems of phase oscillators with asymmetric nonlocal coupling," *Nonlinearity* **33**(2), 611 (2020).
- <sup>36</sup>C. R. Laing and O. Omel'chenko, "Moving bumps in theta neuron networks," *Chaos* **30**(4), 043117 (2020).
- <sup>37</sup>O. E. Omel'chenko, "Traveling chimera states," *J. Phys. A: Math. Theor.* **52**(10), 104001 (2019).
- <sup>38</sup>O. E. Omel'chenko, "Periodic orbits in the Ott–Antonsen manifold," *Nonlinearity* **36**(2), 845 (2022).
- <sup>39</sup>D. Pázó and E. Montbrió, "Low-dimensional dynamics of populations of pulse-coupled oscillators," *Phys. Rev. X* **4**, 011009 (2014).
- <sup>40</sup>J. T. Ariaratnam and S. H. Strogatz, "Phase diagram for the Winfree model of coupled nonlinear oscillators," *Phys. Rev. Lett.* **86**(19), 4278 (2001).
- <sup>41</sup>A. T. Winfree, "Biological rhythms and the behavior of populations of coupled oscillators," *J. Theor. Biol.* **16**(1), 15–42 (1967).
- <sup>42</sup>N. W. Schultheiss, A. A. Prinz, and R. J. Butera, *Phase Response Curves in Neuroscience: Theory, Experiment, and Analysis* (Springer, 2011).
- <sup>43</sup>C. R. Laing, "Phase oscillator network models of brain dynamics," in *Computational Models of Brain and Behavior* (Wiley, 2017), pp. 505–517.
- <sup>44</sup>S. Means and C. R. Laing, "Explosive behaviour in networks of Winfree oscillators," *Chaos, Solitons Fractals* **160**, 112254 (2022).
- <sup>45</sup>O. E. Omel'chenko, M. Wolfrum, S. Yanchuk, Y. L. Maistrenko, and O. Sudakov, "Stationary patterns of coherence and incoherence in two-dimensional arrays of non-locally-coupled phase oscillators," *Phys. Rev. E* **85**(3), 036210 (2012).
- <sup>46</sup>E. A. Martens, C. R. Laing, and S. H. Strogatz, "Solvable model of spiral wave chimeras," *Phys. Rev. Lett.* **104**(4), 044101 (2010).

- <sup>47</sup>J. Xie, E. Knobloch, and H.-C. Kao, "Twisted chimera states and multicore spiral chimera states on a two-dimensional torus," *Phys. Rev. E* **92**, 042921 (2015).
- <sup>48</sup>C. R. Laing, "Chimeras on annuli," *Chaos* **32**(8), 083105 (2022).
- <sup>49</sup>Y. Ding and B. Ermentrout, "Rotating waves of nonlocally coupled oscillators on the annulus," *SIAM J. Appl. Dyn. Syst.* **21**(3), 2047–2079 (2022).
- <sup>50</sup>C. R. Laing, "The dynamics of chimera states in heterogeneous Kuramoto networks," *Physica D* **238**(16), 1569–1588 (2009).

- <sup>51</sup>M. J. Panaggio and D. M. Abrams, "Chimera states on the surface of a sphere," *Phys. Rev. E* **91**(2), 022909 (2015).
- <sup>52</sup>C. R. Laing, "Chimeras in two-dimensional domains: Heterogeneity and the continuum limit," *SIAM J. Appl. Dyn. Syst.* **16**(2), 974–1014 (2017).
- <sup>53</sup>C. R. Laing, "Spiral waves in nonlocal equations," *SIAM J. Appl. Dyn. Syst.* **4**(3), 588–606 (2005).